Supplementary Information

Porous organic polymers based on deep-cavity calixarene for broad-spectrum and high-affinity drug adsorption in gastrointestinal tract

Wei-Yan Chen, Xiao-Min Cao, An-Kang Ying, Yuan-Qiu Cheng, Shu-Xin Zhang, Han-Fei Fu, Yue Li* and Dong-Sheng Guo*

Experimental details

1. Materials and methods

All reagents and starting materials were obtained from commercial suppliers and used without further purification. Predried organic solvents with water content below 0.5% were employed in all procedures. Commercial adsorbents were sourced from certified manufacturers. All drugs used in the experiments were purchased from commercial suppliers and their structures were verified by high-resolution mass spectrometry (HRMS) and ^{1}H NMR.

Materials were characterized as follows: ^{1}H NMR spectra were recorded on a Bruker AVANCE III spectrometer using tetramethylsilane (TMS) as an internal reference; mass spectrometry was performed using an Agilent 6540 TOF spectrometer equipped with an ESI source; FT-IR spectra were acquired on a Thermo Scientific Nicolet iS20 spectrometer; XPS measurements were conducted on a Thermo Scientific ESCALAB 250Xi system; SEM imaging was carried out using a TESCAN MIRA LMS microscope; N_2 physisorption isotherms were measured on a Micromeritics ASAP 2460 analyzer, with specific surface areas calculated using the BET method; zeta potentials were determined using a Malvern Zetasizer Nano ZS90; and UV-Vis spectra for adsorption studies were collected using a Cary 100 spectrophotometer equipped with a 10 mm path length quartz cell and a dual-cell Peltier accessory. In cell-based assays: EdU staining was carried out with a Click-iT EdU kit (Thermo Fisher Scientific), followed by slide scanning on a Nikon Eclipse C1 automated microscope. Cell viability was assessed using a Thermo Scientific Multiskan FC microplate reader.

2. Synthesis

2.1. Tetraformylcalix[4]arene (C4A-CHO). The synthesis of C4A-CHO was performed following a literature procedure with slight modifications.[1] Calix[4]arene (500 mg, 1.2 mmol) and hexamethylenetetramine (urotropine, 6 g, 42.8 mmol) were dissolved in trifluoroacetic acid (40 mL) and heated under reflux for 24 hours under a nitrogen atmosphere with continuous stirring. After cooling to room temperature, the reaction mixture was poured into 1 M HCl (55 mL) and stirred for 15 minutes, CH_2Cl_2 (37 mL) was then added, and stirring was continued overnight. The aqueous layer was extracted with CH_2Cl_2, and the combined organic phases were washed repeatedly with water and dried over anhydrous $MgSO_4$. After removal of the solvent under reduced pressure, the crude product was recrystallized from CH_2Cl_2. Vacuum drying afforded C4A-CHO as a yellow solid. Yield: 69%. ^{1}H NMR (400 MHz, DMSO-d_6) δ: 9.61 (s, 4H, C*H*O), 7.64 (s, 8H, Ar-*H*), 3.89 (d, J = 189.8 Hz, 8H, Ar-CH_2-Ar) (Fig. S1).

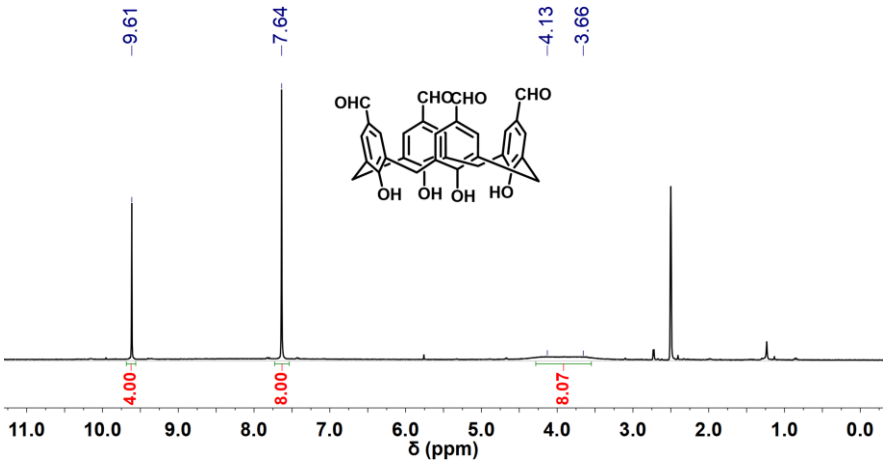

Fig. S1 ^{1}H NMR spectrum of C4A-CHO in DMSO-d_6, 400 MHz, 25 °C.

2.2. Aryldiacetonitrile linkers. All the aryldiacetonitrile linkers except 2,2'-([1,1':4',1'':4'',1'''-quaterphenyl]-4,4'''-diyl)diacetonitrile (QAN) were obtained commercially. The synthesis of QAN was performed according to a previously reported procedure with minor modifications.[2] A mixture of 4,4'-dibromobiphenyl (2.65 g, 7.9 mmol), 4-(cyanomethyl)benzeneboronic acid pinacol ester (0.64 g, 2.64 mmol), sodium carbonate (2.10 g, 19.8 mmol), and $Pd(PPh_3)_4$ (0.23 g, 0.198 mmol) was dissolved in a solvent system of THF (40 mL) and deionized water (10 mL) and refluxed at 80 °C for 24 hours under a nitrogen atmosphere. After cooling to room temperature, the mixture was filtered through a Celite pad and washed thoroughly with THF. The crude product was purified by silica gel column chromatography and subsequently recrystallized from THF. Vacuum drying yielded QAN as a pale yellow solid in 85% yield. ^{1}H NMR (400 MHz, DMSO-d_6) δ: 7.78–7.76 (m, 2H, Ar-*H*), 7.71–7.66 (m, 6H, Ar-*H*), 7.49–7.43 (m, 6H, Ar-*H*), 7.39–7.36 (m, 2H, Ar-*H*), 4.08 (s, 4H, Ar-CH_2-CN).

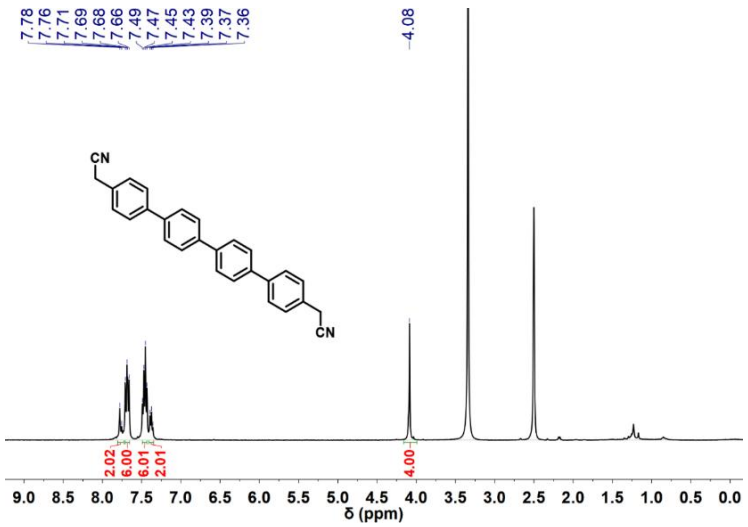

Fig. S2 ^{1}H NMR spectrum of QAN in DMSO-d_6, 400 MHz, 25 °C.

2.3. Olefin-linked C4A-based POPs. C4A-CHO (10 mg, 0.019 mmol) and TAN (11.7 mg, 0.038 mmol) were dissolved in a mixed solvent system comprising 1,4-dioxane (0.2 mL), methanol (0.2 mL), THF (0.2 mL), and DMF (0.3 mL) via sonication, and the solution was transferred to a borosilicate glass tube. After adding 4 M aqueous KOH solution (0.1 mL), the tube was subjected to three freeze–pump–thaw cycles and sealed under vacuum. The sealed tube was heated at 150 °C for 3 days. Upon completion, the reaction mixture was cooled

to room temperature, and the resulting solid was isolated by centrifugation, followed by thorough washing with THF and water. The product was solvent exchanged 4–5 times with fresh THF. After drying in vacuum, C4A-TAN was obtained as a yellow solid in 63% yield.

The synthesis of C4A-PAN, C4A-BAN, and C4A-QAN followed a similar procedure, with the respective linkers—1,4-phenylenediacetonitrile (PAN), biphenyldiacetonitrile (BAN), and 2,2'-([1,1':4',1'':4'',1'''-quaterphenyl]-4,4'''-diyl)diacetonitrile (QAN)—used in place of QAN. The yields of these POPs were 35%, 55%, and 60%, respectively.

2.4. Azo-linked C4A-based POPs. In a typical polymerization procedure, tetranitrocalix[4]arene (C4A-NO_2, 0.200 g, 0.33 mmol; synthesized as described in Ref. 3 and characterized in Fig. S4), 4,4''-diaminoterphenyl (DATP, 0.172 g, 0.66 mmol), KOH (0.186 g, 3.31 mmol), and DMF (15 mL) were added to a Schlenk tube. The mixture was degassed via three freeze–pump–thaw cycles and subsequently heated at 150 °C for 24 hours. After cooling to room temperature, the resulting solid was collected by centrifugation and washed sequentially with DMF, THF, water, and ethanol. The product, denoted as C4A-N=N-TP, was then dried under vacuum at 55 °C for 16 hours to yield a brown solid. The successful formation of the azo linkage was confirmed by FT-IR spectroscopy.

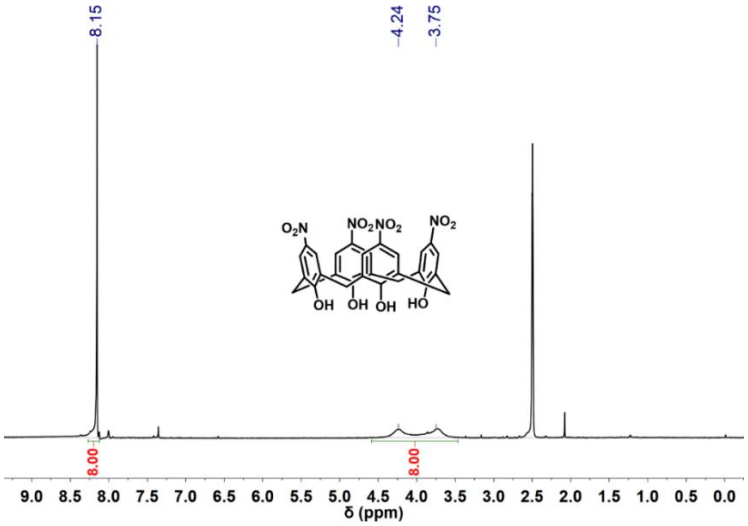

Fig. S3 ^{1}H NMR spectrum of C4A-NO_2 in DMSO-d_6, 400 MHz, 25 °C.

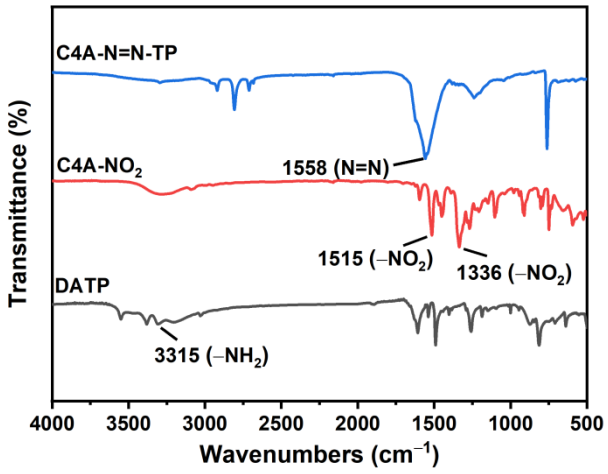

Fig. S4 FT-IR spectrum of C4A-N=N-TP. The spectra for the monomers are given for comparison.

2.5. Imine-linked C4A-based POPs. According to Ref. 4, a solution of C4A-CHO (0.022 mmol, 12.0 mg) in chloroform (5 mL) and methanol (0.25 mL) was placed in a glass vial and carefully overlaid with 5.0 mL of water to establish an oil–water interface. An aqueous solution (6 mL) containing DATP (0.046 mmol, 12 mg), acetonitrile (0.50 mL), and acetic acid (0.50 mL) was added dropwise to the aqueous phase. The vial was sealed and kept undisturbed at room temperature for 3 days, resulting in the formation of a bright orange powder (denoted as C4A-C=N-TP) at the interface. The successful formation of the imine linkage was confirmed by FT-IR spectroscopy.

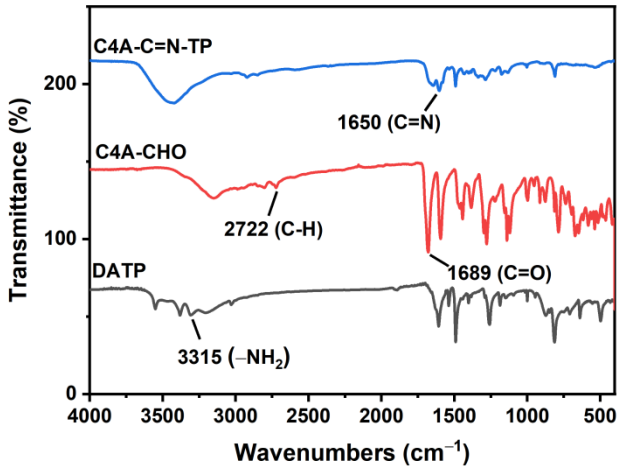

Fig. S5 FT-IR spectrum of C4A-C=N-TP. The spectra for the monomers are given for comparison.

2.6. Soluble analogs of the binding sites of olefin-linked C4A-based POPs. To simulate the binding sites of olefin-linked C4A-based POPs, C4A was functionalized with –COOH and −CH=C(CN)PhCOOH to obtain soluble analogs (denoted as C4A-COOH and C4A-CH=C(CN)PhCOOH, respectively) for measuring binding constants in homogeneous solution.

The synthesis of C4A-COOH was carried out according to Ref. 5 as follows: C4A-CHO (381 mg, 0.710 mmol) and NaH_2PO_4 (85 mg, 0.710 mmol) were dissolved in a mixed solvent of DMSO (7.1 mL) and water (1 mL). After dropwise addition of 6 mL aqueous NaClO solution (1 M) over 3 hours, the mixture was stirred overnight at room temperature and then acidified with 5 M HCl. The resulting precipitate was collected by filtration, washed thoroughly with water, and dried to afford C4A-COOH as a light yellow solid (368 mg, 86% yield). ^{1}H NMR (400 MHz, DMSO-d_6) δ: 7.71 (s, 8H, Ar-*H*), 4.01 (s, 8H, Ar-CH_2-Ar).

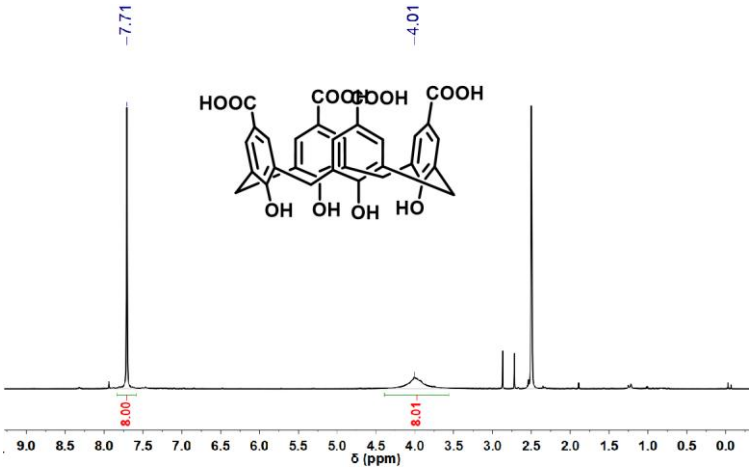

Fig. S6 ^{1}H NMR spectrum of C4A-COOH in DMSO-d_6, 400 MHz, 25 °C with trifluoroacetic acid.

C4A-CH=C(CN)PhCOOH was synthesized by reacting C4A-CHO (100 mg, 0.187 mmol), 4-(cyanomethyl)benzoic acid (130 mg, 0.81 mmol), and piperidine (4.9 µL, 0.05 mmol) in methanol (20 mL) at 50 °C for 3 days. Reaction progress was monitored by thin-layer chromatography. The mixture was then concentrated under reduced pressure, and the crude product was isolated by filtration. After dialysis, the target compound was obtained as a yellowish-brown solid in 45% yield. ^{1}H NMR (400 MHz, DMSO- d_6) δ: 7.79 (d, J = 7.2 Hz, 8H, Ar-*H*), 7.62 (d, J = 13.8 Hz, 8H, Ar-*H*), 7.52 (s, 4H, calix-*H*), 7.50 (s, 4H, calix-*H*). ESI-MS m/z: 1107.28 $[M - H]^-$, 553.14 $[M - 2H]^{2-}$.

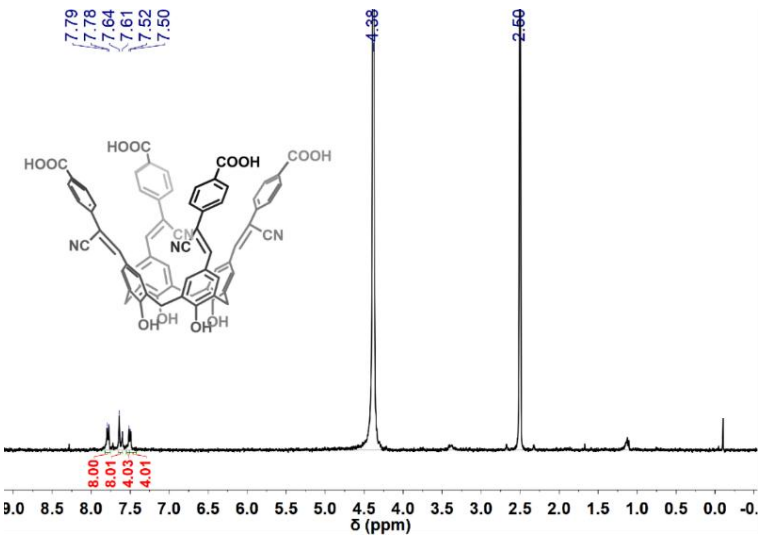

Fig. S7 ^{1}H NMR spectrum of C4A-CH=C(CN)PhCOOH.

2.7. Cy5-labeled C4A-TAN. At 0 °C, C4A-TAN (2 g) was added in portions to a solution of $LiAlH_4$ (760 mg, 2 equiv) in anhydrous THF (40 mL). The reaction mixture was allowed to warm to room temperature and stirred for 3 days. Upon completion, the reaction was carefully quenched by successive addition of water (0.8 mL), 15% NaOH aqueous solution (2.4 mL), and additional water (0.8 mL), followed by vigorous stirring for 30 minutes. The solid was isolated by filtration, washed with ethyl acetate (30 mL), and dried to afford the intermediate. The resulting solid (1 g) was then reacted with EDC·HCl (1.0 mM, 50 mL) and Sulfo-NHS (1.0 mM, 20 mL) in aqueous suspension. After stirring for 30 minutes, an aqueous solution of Cy5-COOH (5.2 mg, 0.01 mmol) was added, and the mixture was stirred in the dark for 12 h. The solid was collected by centrifugation, washed with ethyl acetate, and stirred in a methanol–water mixture for an additional 12 h. The final Cy5-labeled C4A-TAN was obtained after lyophilization for 8 hours followed by vacuum drying.

3. *In v*itro adsorption experiments

The adsorption performance was evaluated in simulated intestinal fluid (SIF). In a typical procedure, 1.5 mg of POP was dispersed in 4 mL of drug solution in SIF (concentration range: 40–200 mg L^{-1}) and stirred for 3 hours to reach adsorption equilibrium. After centrifugation at 15,000 rpm for 10 minutes, the supernatant was filtered through a 0.22 µm membrane. The drug concentration in the filtrate was determined by UV-Vis spectrophotometry at the maximum absorption wavelength of each drug (λ = 370 nm for IRI, 220 nm for PTX, and 486 nm for DOX). The adsorption capacity was calculated as:

$$q_t = \frac{(C_0 - C_t) \cdot V \cdot M}{m} \quad \text{(S1)}$$

where C_0 and C_t represent the initial and equilibrium concentrations of the drug in solution, respectively; V is the solution volume; M is the molecular weight of the drug; and m is the mass of the adsorbent.

To characterize adsorption thermodynamics, the adsorption isotherm data were fitted using the Langmuir (Equation S2), Freundlich (Equation S3), Sips (Equation S4), and Redlich-Peterson (Equation S5) models:

$$q_e = \frac{Q_{max} \cdot K_L \cdot C_e}{1 + K_L \cdot C_e} \quad \text{(S2)}$$

$$q_e = K_F \cdot (C_e / C^{\ominus}) \quad \text{(S3)}$$

$$q_e = \frac{q_m (K_S \cdot C_e)^{m_S}}{1 + (K_S \cdot C_e)^{m_S}} \quad \text{(S4)}$$

$$q_e = \frac{K_{RP} \cdot C_e}{1 + a_{RP} \cdot C_e{}^{g}} \quad \text{(S5)}$$

where q_e is the equilibrium adsorption capacity; Q_{max} is the maximum adsorption capacity; C_e is the equilibrium concentration of the adsorbate; K_L is the Langmuir constant related to adsorption affinity; K_F is the Freundlich constant; $C^{\ominus}$ is the standard concentration (1 M) and n is the Freundlich exponent related to adsorption intensity; q_m is the maximum monolayer adsorption capacity; K_S is the Sips affinity constant; m_S is the dimensionless heterogeneity index; K_{RP} is the Redlich-Peterson constant related to adsorption capacity; a_{RP} is a constant related to adsorption energy; and g is the dimensionless exponent.

To evaluate the adsorption kinetics, the adsorption capacity (q_t) of the POP after contact with the drug solution for specified time intervals was measured and fitted using the pseudo-first-order (Equation S6) and pseudo-second-order (Equation S7) kinetic models:

$$\ln(q_e - q_t) = \ln q_e - k_1 \cdot t \quad \text{(S6)}$$

$$\frac{t}{q_t} = \frac{1}{k_2 \cdot q_e{}^{2}} + \frac{t}{q_e} \quad \text{(S7)}$$

where k_1 and k_2 represent the rate constants of the pseudo-first-order and pseudo-second-order kinetic models, respectively.

4. Measurement of host–guest binding constants (K_as)

The K_as of C4A-COOH and C4A-CH=C(CN)PhCOOH toward DOX were determined by direct fluorescence titration. Changes in emission intensity were recorded upon incremental addition of the host into a solution of DOX (0.50 μM) in SIF.

For IRI and PTX, the K_a values of C4A-CH=C(CN)PhCOOH were obtained via competitive fluorescence titration using rhodamine B (RhB) as the reporter dye. First, the K_a between C4A-CH=C(CN)PhCOOH and RhB was measured by direct fluorescence titration under conditions analogous to those used for DOX. Competitive titrations were then performed by gradually introducing the competitor (IRI or PTX) into solutions containing the preformed reporter pair (0.50 μM RhB and 0.50 μM C4A-CH=C(CN)PhCOOH).

The K_as of C4A-COOH toward IRI and PTX were similarly assessed by competitive fluorescence titration, but with methylene blue (MB) as the fluorescent reporter, owing to the weak affinity of C4A-COOH for RhB. The concentrations of C4A-COOH and MB in the competitive titration were 2.0 and 0.8 μM, respectively.

Fluorescence titration data from both direct and competitive experiments were fitted nonlinearly based on a 1:1 binding model. The fitting modules were obtained from the website of Prof. Nau's research group (http://www.jacobsuniversity.de/ses/wnau) under the "Fitting Functions" section.

5. Cell culture and toxicity assessment

MODE-K cells were obtained from the Cell Bank of the Chinese Academy of Sciences (Shanghai, China). The cells were cultured in DMEM supplemented with 10% FBS and 1% penicillin/streptomycin. At 70–80% confluence, the cells were detached using trypsin solution and incubated for 5 minutes. After centrifugation at 1000 rpm for 5 minutes, the supernatant was removed. Fresh serum-containing medium (3 mL) was added

to neutralize residual trypsin. The cells were then resuspended in serum-supplemented medium and incubated at 37 °C and 5% CO_2.

The cytotoxicity of various materials toward MODE-K cells was evaluated using the CCK-8 assay. Approximately 5,000 cells per well were seeded in a 96-well plate and incubated for 12 hours to allow complete adhesion. The cells were then treated with different concentrations (0.05–1 mg·mL^{-1}) of C4A-TAN or MAC, and incubated for 24 hours in normoxia. After treatment, the medium was aspirated and replaced with a mixture of 10 μL CCK-8 reagent and 90 μL fresh medium. Following an additional 2-hour incubation, the absorbance at 450 nm was measured using a microplate reader. Cell viability was calculated according to the following formula:

$$\text{Cell viability } (\%) = \frac{\text{OD}_{\text{sample}} - \text{OD}_{\text{blank}}}{\text{OD}_{\text{control}} - \text{OD}_{\text{blank}}} \times 100\% \quad \text{(S6)}$$

where OD_{sample}, $OD_{control}$, and OD_{blank} represent the absorbance values of sample-treated cells, untreated cells, and cell-free medium, respectively. All experiments were performed with five independent replicates.

6. *In vivo* murine studies

6.1. Mice. Female BALB/c mice (6–8 weeks old) were obtained from Henan Skobes Biotechnology Co., Ltd. All animal experiments were conducted in compliance with the Chinese Regulations for the Administration of Affairs Concerning Experimental Animals (Tianjin, revised in June 2004) and the Guiding Principles in the Care and Use of Animals of the American Physiological Society. The study protocol was approved by the Animal Ethical and Welfare Committee (AEWC) of Radiation Medicine (Tianjin, China) (Approval No. ZXHK-DWLL-2025-0109).

6.2. Biodistribution of POPs tracked by fluorescence labeling. After one week of acclimation, healthy mice were orally administered a deionized water suspension of Cy5-labeled C4A-TAN at a dose of 750 mg kg^{-1}. The animals were euthanized at 1, 3, 6, 12, 18, and 24 hours post-administration. Major organs, including the gastrointestinal tract, heart, liver, spleen, lungs, and kidneys, were collected. Fluorescence distribution in each organ was visualized and recorded using a small-animal in vivo imaging system.

6.3. Complete blood count and blood biochemistry analysis. Mice in the experimental group were administered a deionized water suspension of C4A-TAN by oral gavage at a dose of 750 mg kg^{-1}, whereas control group mice received an equal volume of sterile normal saline (n = 5 per group). All animals were euthanized 6 h post-administration, and blood samples were collected from both groups for complete blood count and blood biochemical analysis.

To evaluate the chronic toxicity of this POP, the administration period for mice was extended to 28 days. The mice received a daily dose of 750 mg kg^{-1} of C4A-TAN (uniformly suspended in deionized water) or an equivalent volume of saline via oral gavage. Blood samples were collected from the C4A-TAN-treated group on day 14 (midpoint) and from both groups on day 28 (endpoint) for complete blood count and blood biochemical analysis.

6.4. Evaluation of the potency of C4A-TAN for treating chemotherapy-induced gastrointestinal mucositis. IRI and PTX were selected as representative chemotherapeutic agents, with medicinal activated charcoal (MAC) serving as the positive control. For each drug, female BALB/c mice (4–6 weeks old) were allocated into four groups (n = 5 per group) and acclimatized for one week prior to experimentation. Group 1 served as the blank control and received 200 μL of normal saline via injection. Group 2 was administered IRI (70 mg kg^{-1}, twice daily) or PTX (15 mg kg^{-1}, once every two days). Groups 3 and 4 received the same chemotherapeutic regimen as Group 2, but were orally administered an aqueous suspension of C4A-TAN (750 mg kg^{-1}) or MAC (750 mg kg^{-1}), respectively, 90 min before each drug injection. Body weight and diarrhea severity were monitored daily throughout the experimental period.

On day 10 (for IRI) or day 14 (for PTX), all mice were injected with EdU (80 mg kg^{-1}) and euthanized 4 hours later. The intestinal tract was excised, and its length was measured. For EdU staining, intestinal samples were fixed in paraformaldehyde, embedded in paraffin, and sectioned at 4 μm thickness. After

dewaxing, sections were stained using a Click-iT EdU kit, and nuclei were counterstained with DAPI. Stained slides were scanned using an automated slide scanner.

Data are presented as the mean ± standard deviation (s.d.). Statistical analysis of data was performed with one or two-way analysis of variance (ANOVA) for comparison of multiple groups using the GraphPad Prism 8.0 software. The level of significance was defined at $*p < 0.05$, $**p < 0.01$ and $***p < 0.001$.

6.5. Dose-response study. A mouse model of intestinal mucositis was established using IRI or PTX at the doses indicated above. Mice were then randomly divided into the following groups ($n = 5$ per group): a model control group (administered an equal volume of sterile saline) and C4A-TAN treatment groups (150, 300, 450, 600, 750, and 900 mg kg^{-1}, suspended in deionized water). C4A-TAN was administered orally by gavage 90 minutes prior to each drug injection. Diarrhea in the mice was monitored daily and scored using a 4-point clinical scale: 0, normal; 1, mild (soft stool); 2, moderate (unformed stool); and 3, severe (watery stool). The mean diarrhea score for each group served as the primary efficacy endpoint for statistical analysis.

Supporting figures

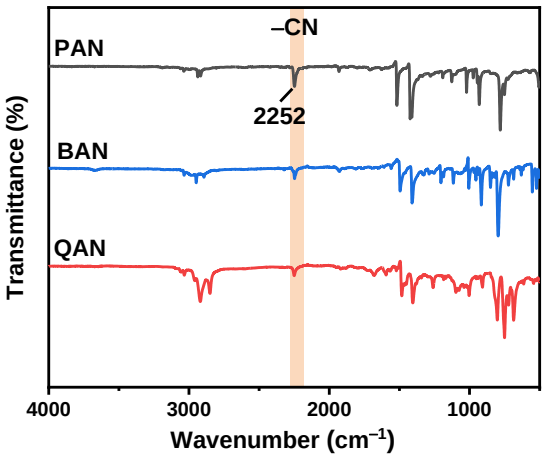

Fig. S8 FT-IR spectra of PAN, BAN, and QAN.

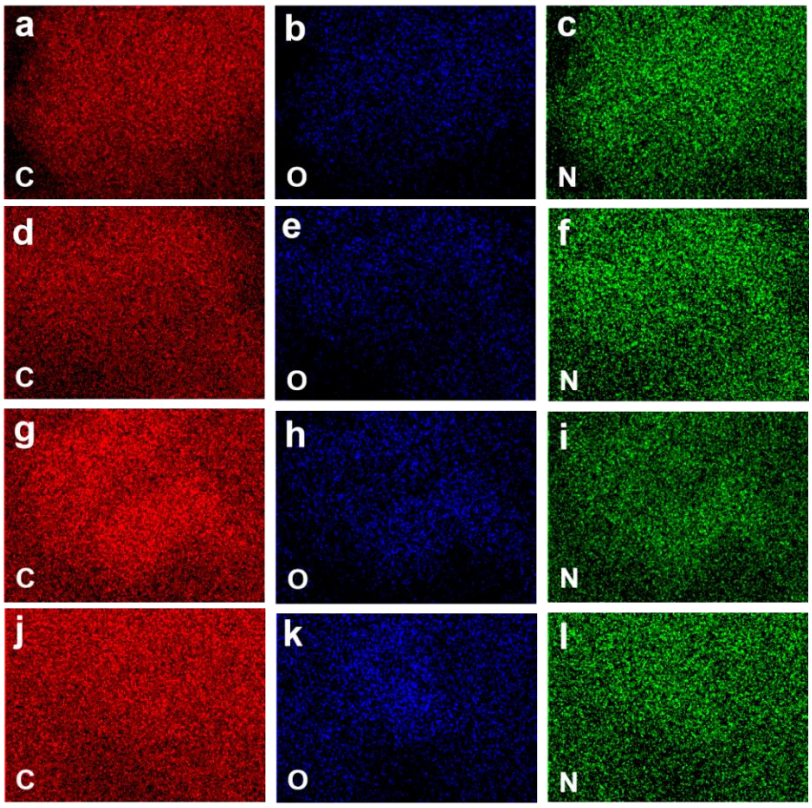

Fig. S9 EDS elemental mapping of olefin-linked C4A-based POPs: (a–c) C4A-PAN, (d–f) C4A-BAN, (g–i) C4A-TAN, and (j–l) C4A-QAN.

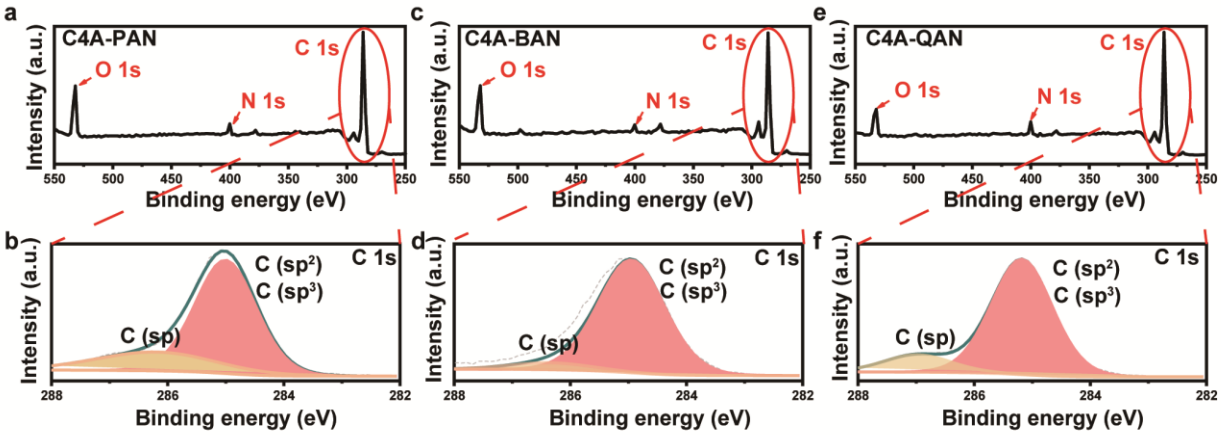

Fig. S10 XPS spectra of (a,b) C4A-PAN, (c,d) C4A-BAN, and (e,f) C4A-QAN: (a,c,e) full view; (b,d,f) C 1s.

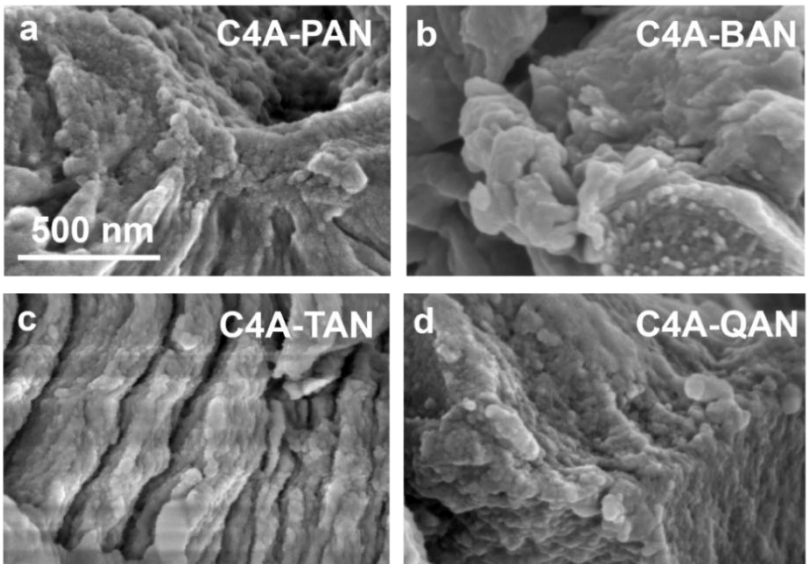

Fig. S11 SEM images of (a) C4A-PAN, (b) C4A-BAN, (c) C4A-TAN, and (d) C4A-QAN. Scale bar: 500 nm.

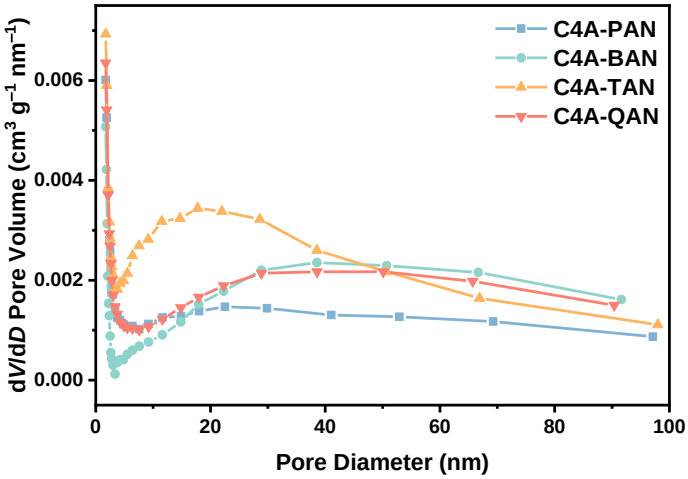

Fig. S12 BJH pore size distributions of olefin-linked C4A-based POPs.

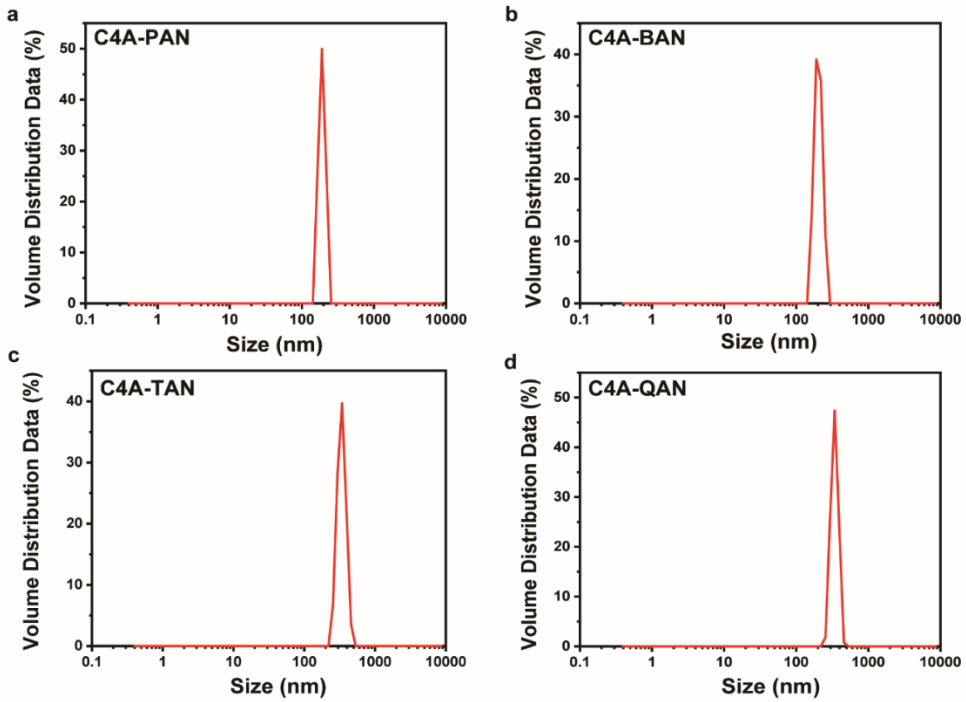

Fig. S13 DLS profiles of (a) C4A-PAN, (b) C4A-BAN, (c) C4A-TAN, and (d) C4A-QAN.

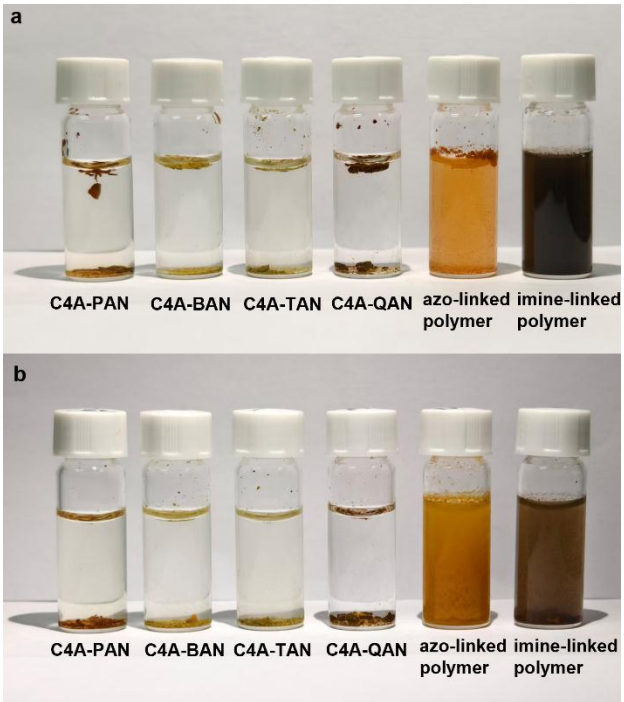

Fig. S14 Photographs of the C4A-based POPs (10 mg) after shaking in 3 mL of (a) SGF and (b) SIF at 37 °C for 24 h.

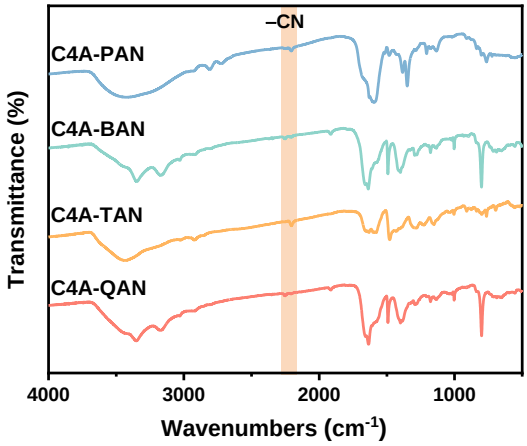

Fig. S15 FT-IR spectra of the olefin-linked C4A-based POPs after the subsequent incubation in SGF (24 h) and SIF (24 h).

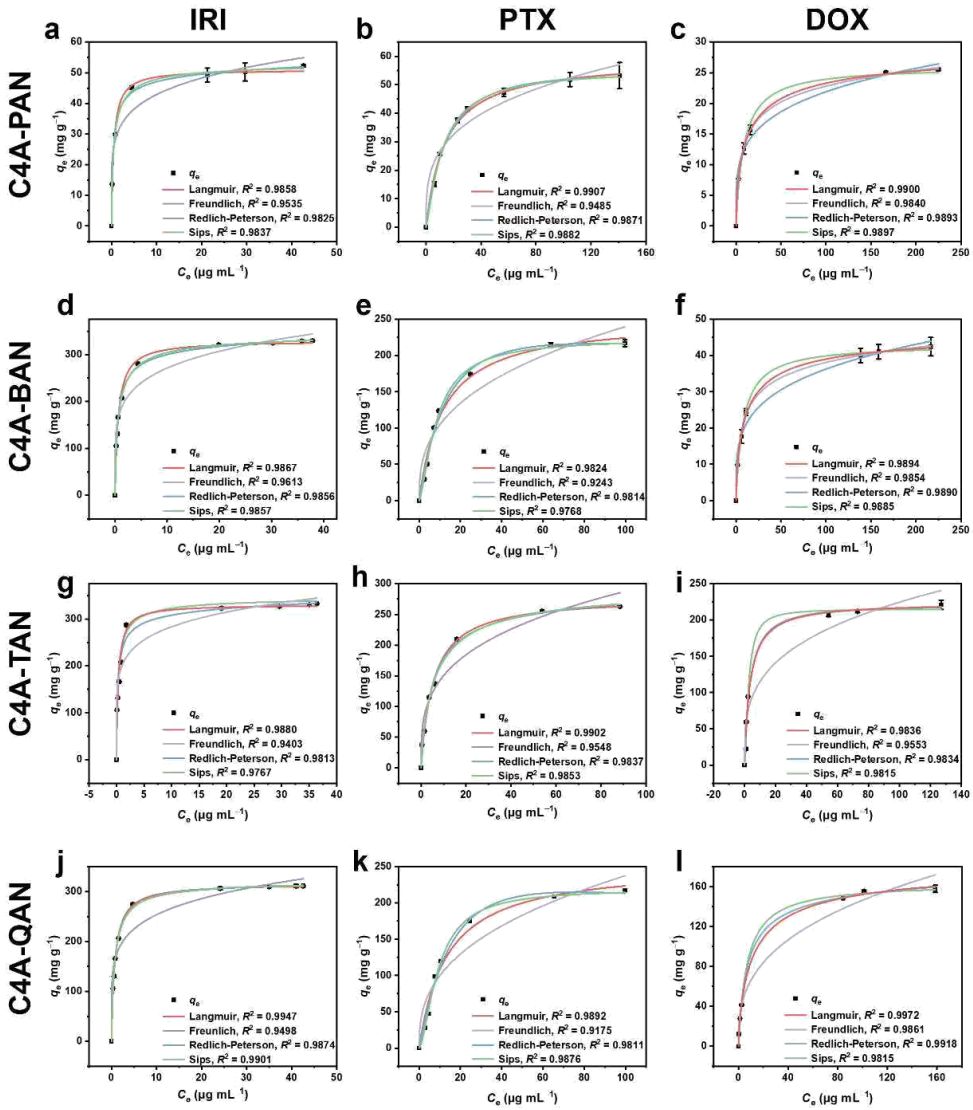

Fig. S16 Adsorption isotherms of IRI (a, d, g, j), DOX (b, e, h, k), and PTX (c, f, i, l) on C4A-PAN (a–c), C4A-BAN (d–f), C4A-TAN (g–i), and C4A-QAN (j–l) fitted with different models.

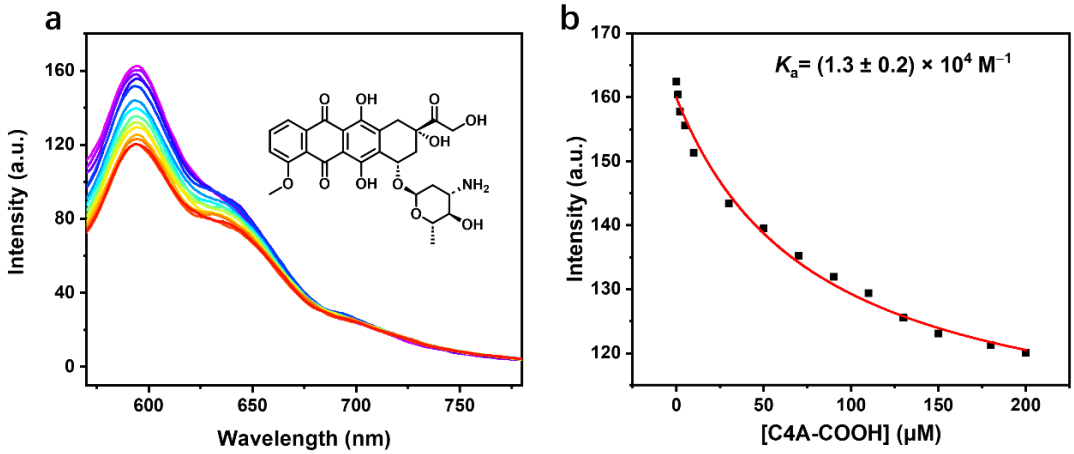

Fig. S17 (a) Direct fluorescence titration of DOX (0.5 μM) with C4A-COOH (up to 120.0 μM) in SIF (pH = 7.0) at 25 °C, λ_{ex} = 540 nm. (b) Associated titration curve at λ_{em} = 595 nm was fitted according to the 1:1 binding stoichiometry.

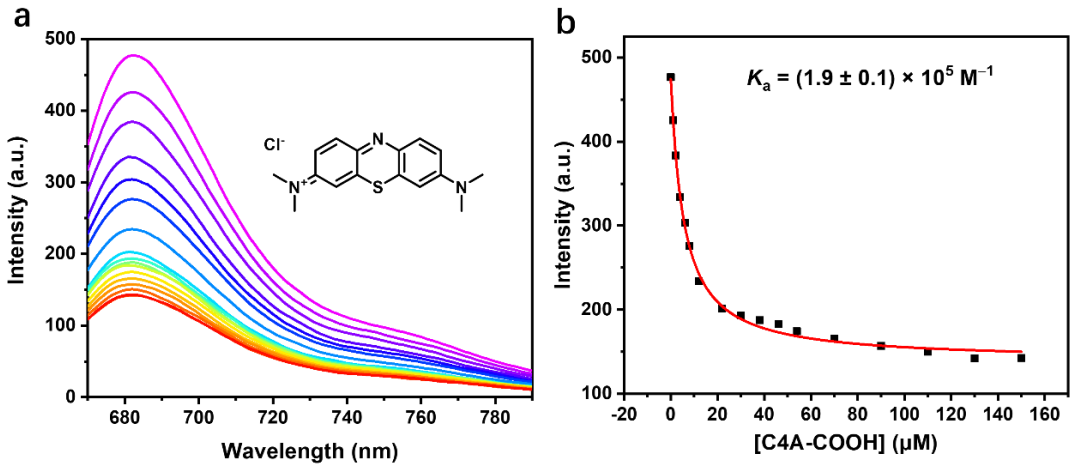

Fig. S18 (a) Direct fluorescence titration of MB (0.8 mM) with C4A-COOH (up to 150.0 mM) in SIF (pH = 7.0) at 25 °C, λ_{ex} = 640 nm. (b) Associated titration curve at λ_{em} = 683 nm was fitted according to the 1:1 binding stoichiometry.

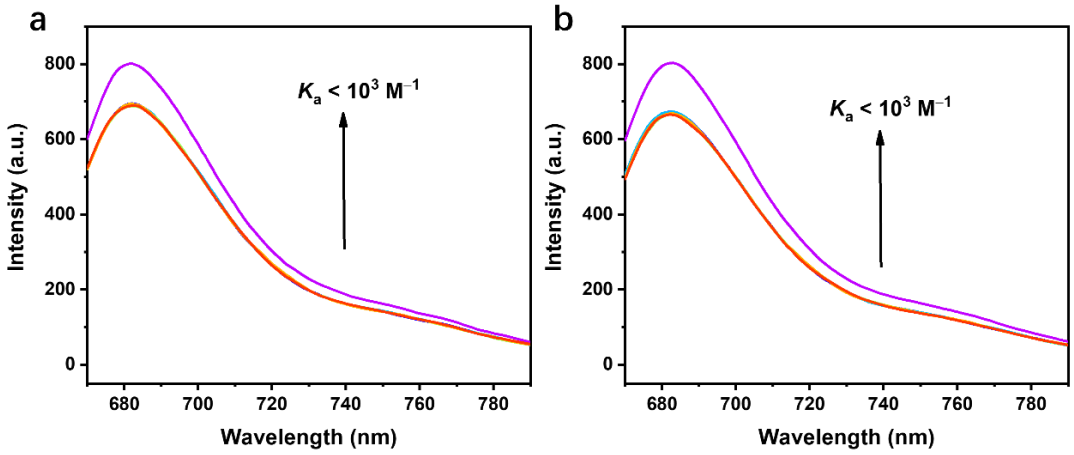

Fig. S19 Competitive fluorescence titration of (a) IRI (0–80.0 μM) and (b) PTX (0–80.00 μM) against the C4A-COOH/MB (2.0/0.8 μM) host–dye pair in SIF (pH 7.0, 25°C; λ_{ex} = 640 nm). The top curves represent the fluorescence spectra of the MB dye in the absence of either C4A-COOH or competitor drugs.

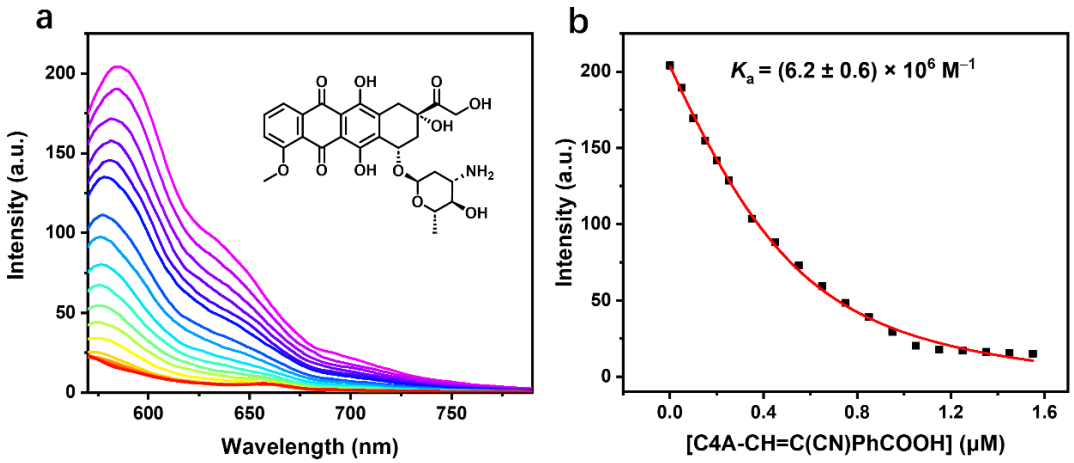

Fig. S20 (a) Direct fluorescence titration of DOX (0.5 μM) with C4A-CH=C(CN)PhCOOH (up to 1.55 μM) in SIF (pH = 7.0) at 25 °C, λ_{ex} = 540 nm. (b) Associated titration curve at λ_{em} = 595 nm was fitted according to the 1:1 binding stoichiometry.

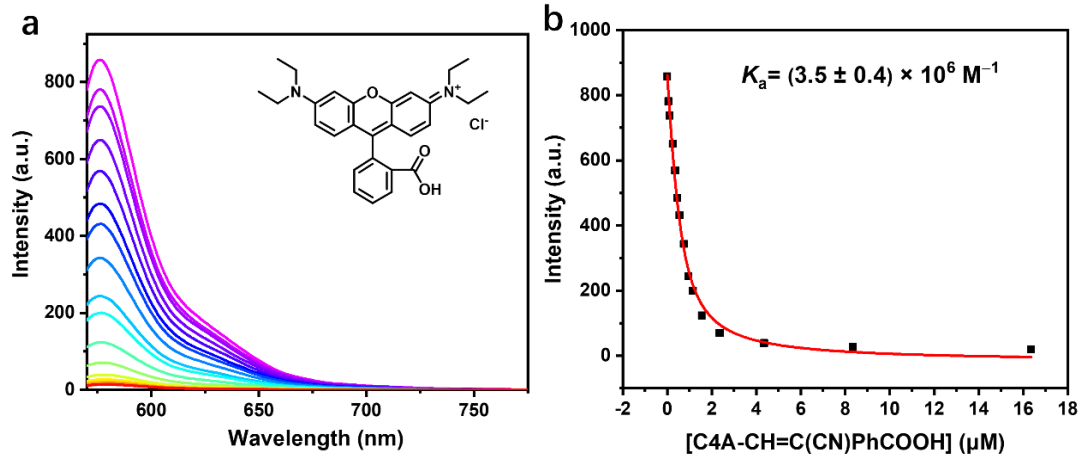

Fig. S21 (a) Direct fluorescence titration of RhB (0.5 μM) with C4A-CH=C(CN)PhCOOH (up to 16.4 μM) in SIF (pH = 7.0) at 25 °C, λ_{ex} = 554 nm. (b) Associated titration curve at λ_{em} = 575 nm was fitted according to the 1:1 binding stoichiometry.

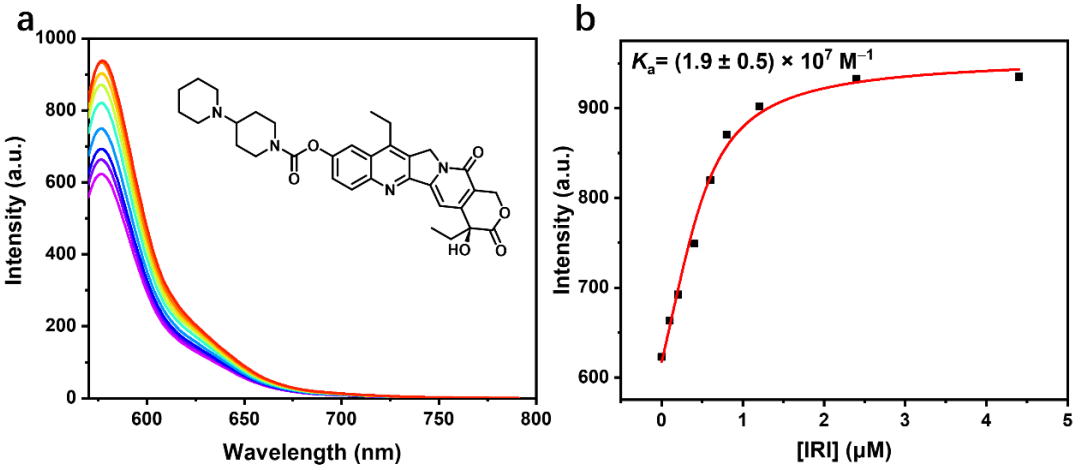

Fig. S22 (a) Competitive fluorescence titration of C4A-CH=C(CN)PhCOOH/RhB (0.5/0.5 μM) host–dye pair with IRI (up to 4.4 μM) in SIF (pH = 7.0) at 25 °C, λ_{ex} = 554 nm. (b) Associated titration curve at λ_{em} = 575 nm was fitted according to the 1:1 competitive binding model.

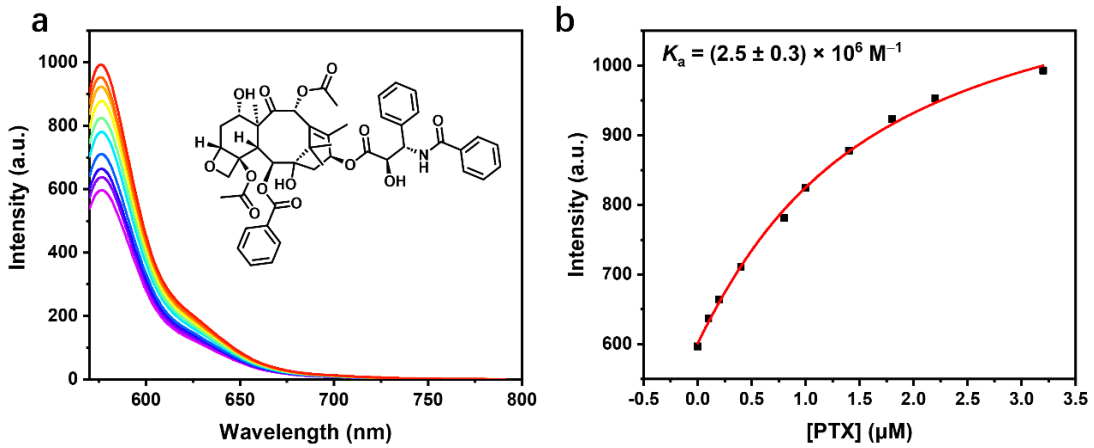

Fig. S23 (a) Competitive fluorescence titration of C4A-CH=C(CN)PhCOOH/RhB (0.5/0.5 μM) host–dye pair with PTX (up to 3.2 μM) in SIF (pH = 7.0) at 25 °C, λ_{ex} = 554 nm. (b) Associated titration curve at λ_{em} = 575 nm was fitted according to the 1:1 competitive binding model.

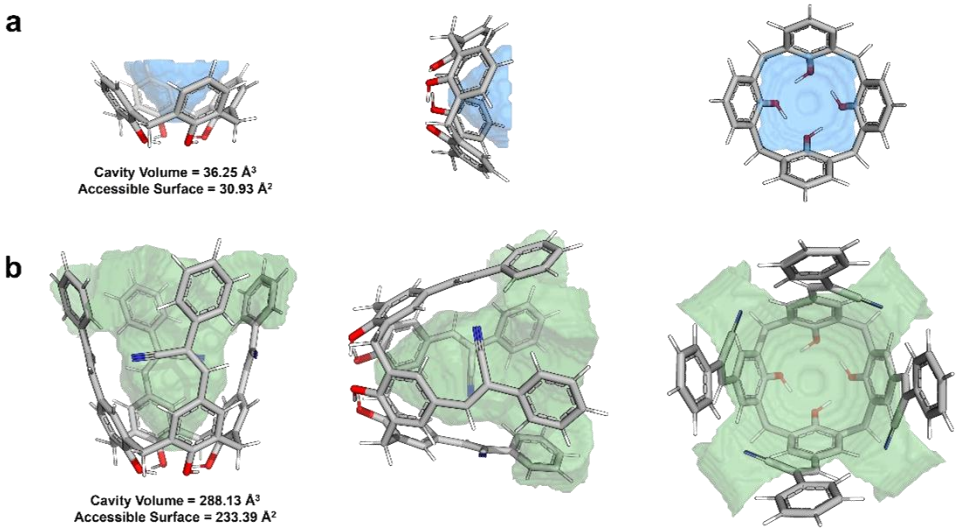

Fig. S24 Cavity conformations of the calixarene host: (a) unfunctionalized C4A and (b) −CH=C(CN)Ph-functionalized C4A. From left to right: side view, tilted view, and top view. The calculation was conducted using the MoloVol (version 1.2.0) program with the two-probe mode enabled.[6] A small probe radius of 0.8 Å was used to map the internal cavity surface, while a large probe radius of 5.0 Å defined the effective pocket boundary for the open cavity system. The grid resolution was set to 0.18 Å. The cavity volumetric maps were visualized in PyMOL.

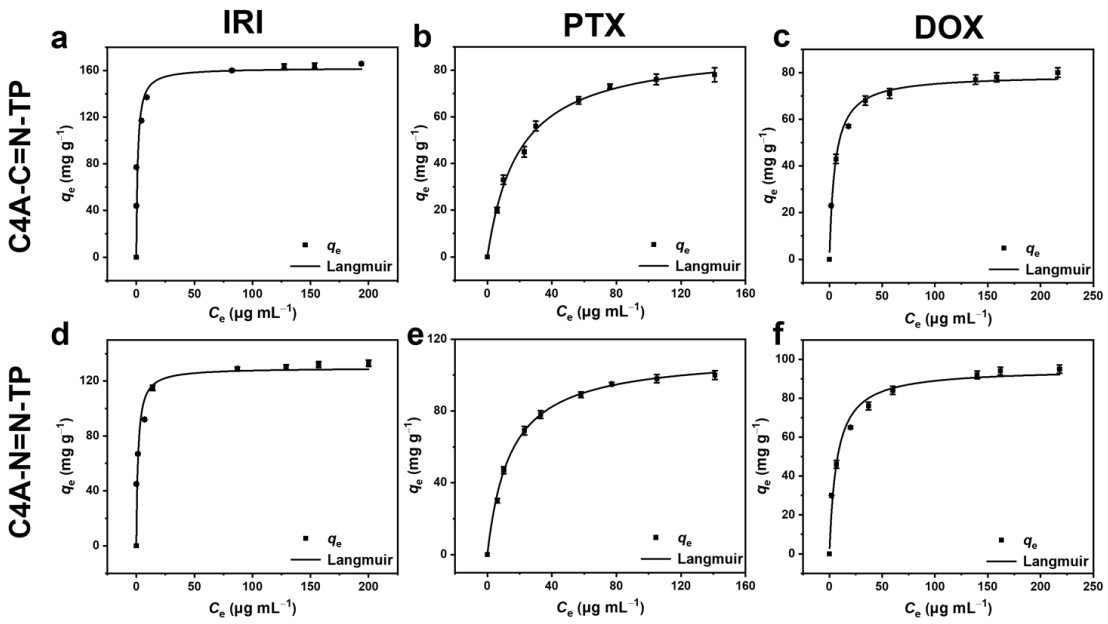

Fig. S25 Thermodynamic fitting of the adsorption isotherms for (a, d) IRI, (b, e) PTX, and (c, f) DOX on (a, c, e) C4A-C=N-TP and (b, d, f) C4A-N=N-TP.

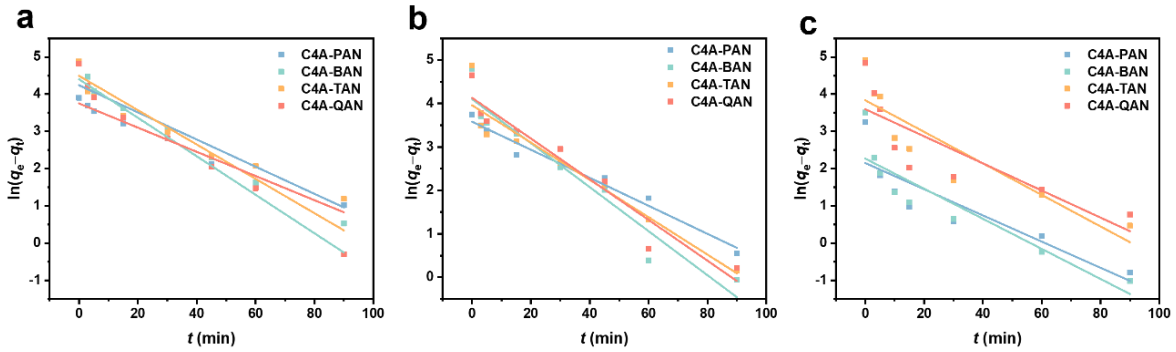

Fig. S26 Pseudo-first-order kinetic modeling for the adsorption of (a) IRI, (b) PTX, and (c) DOX by olefin-linked C4A-based POPs.

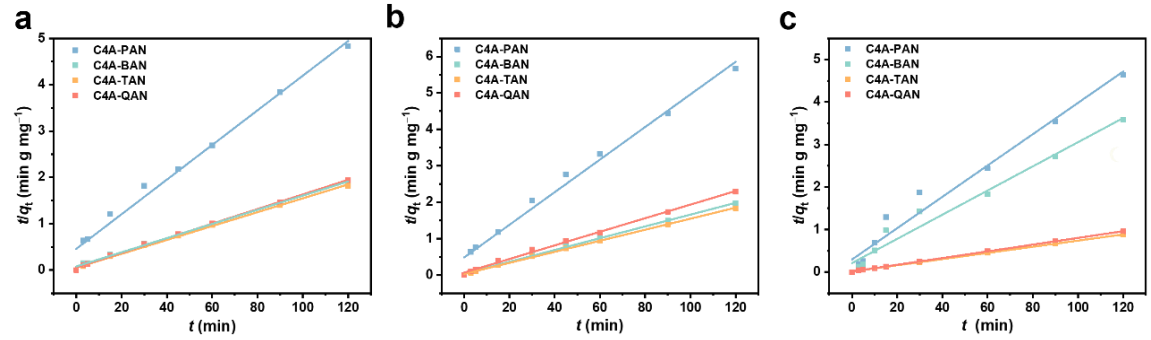

Fig. S27 Pseudo-second-order kinetic modeling for the adsorption of (a) IRI, (b) PTX, and (c) DOX by olefin-linked C4A-based POPs.

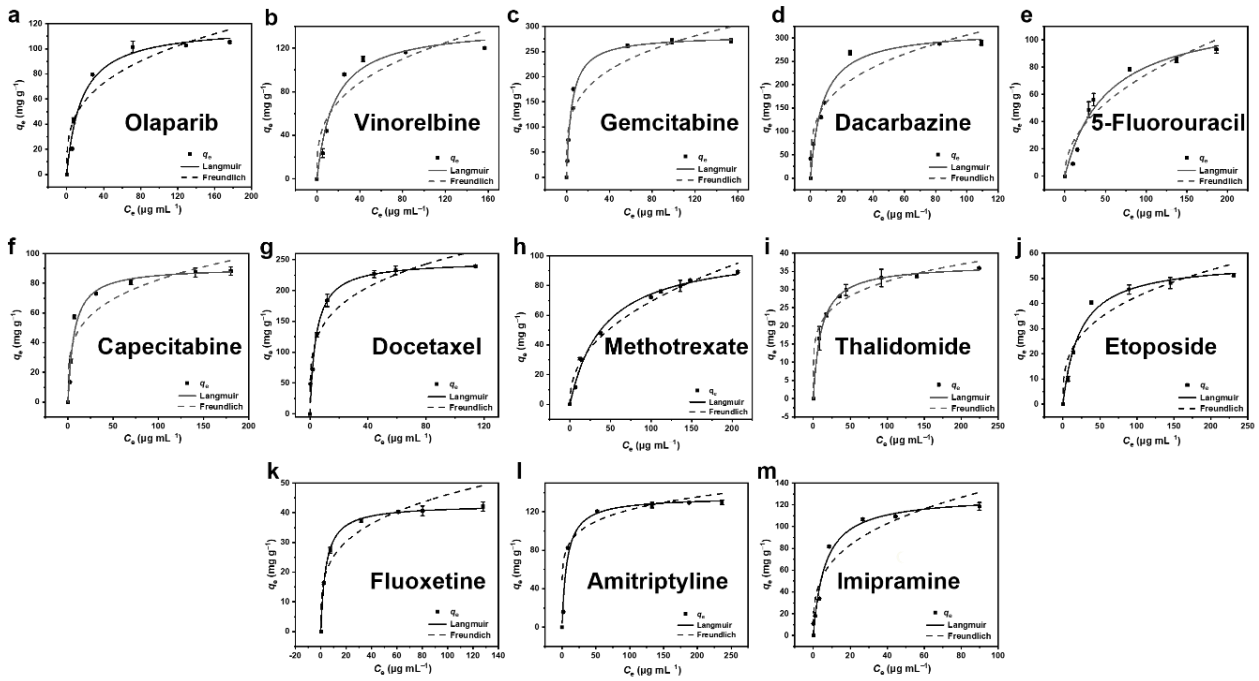

Fig. S28 Equilibrium adsorption capacities and corresponding thermodynamic fitting of adsorption isotherms for C4A-TAN toward the following drugs: (a) olaparib, (b) vinorelbine, (c) gemcitabine, (d) dacarbazine, (e) 5-fluorouracil, (f) capecitabine, (g) docetaxel, (h) methotrexate, (i) thalidomide, (j) etoposide, (k) fluoxetine, (l) amitriptyline and (m) imipramine.

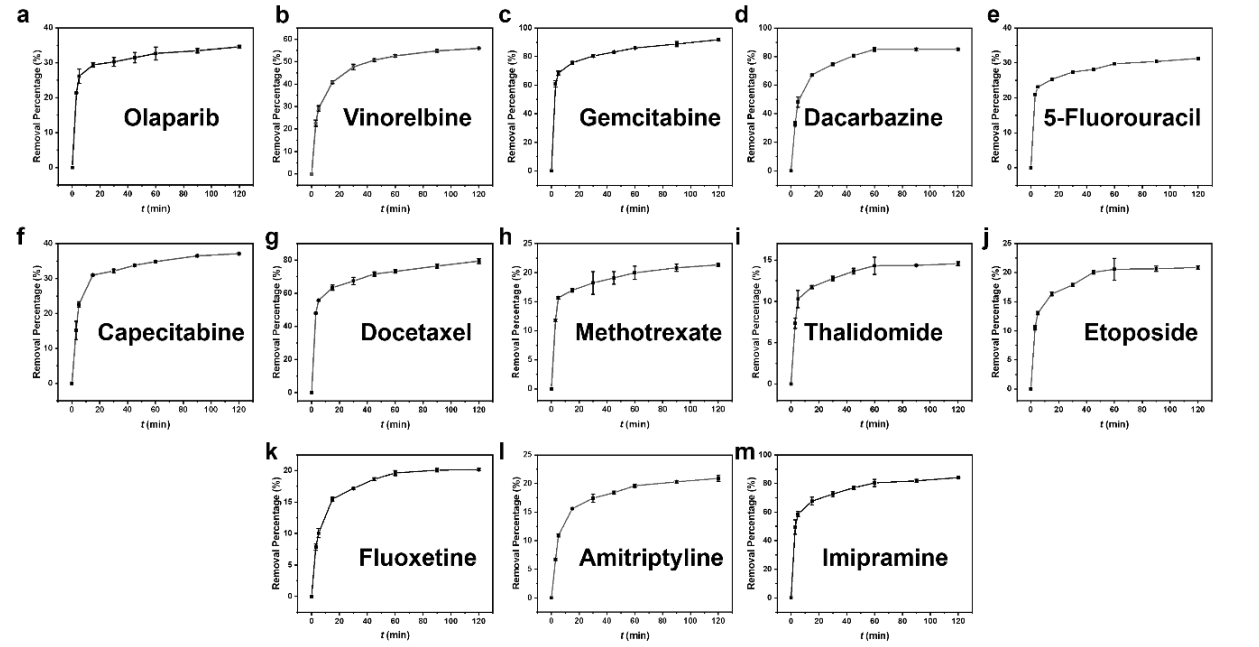

Fig. S29 Time-dependent adsorption profiles of C4A-TAN toward (a) olaparib, (b) vinorelbine, (c) gemcitabine, (d) dacarbazine, (e) 5-fluorouracil, (f) capecitabine, (g) docetaxel, (h) methotrexate, (i) thalidomide, (j) etoposide, (k) fluoxetine, (l) amitriptyline and (m) imipramine.

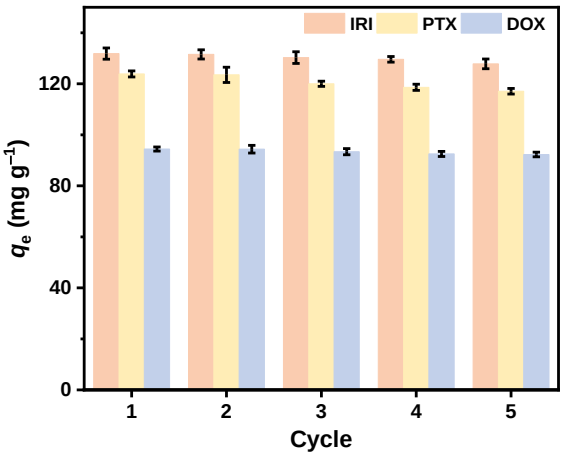

Fig. S30 Adsorption capacities of C4A-TAN (0.375 mg mL^{-1}) toward IRI, PTX, and DOX (initial concentration: 50 μg mL^{-1} each) over five consecutive adsorption–desorption cycles.

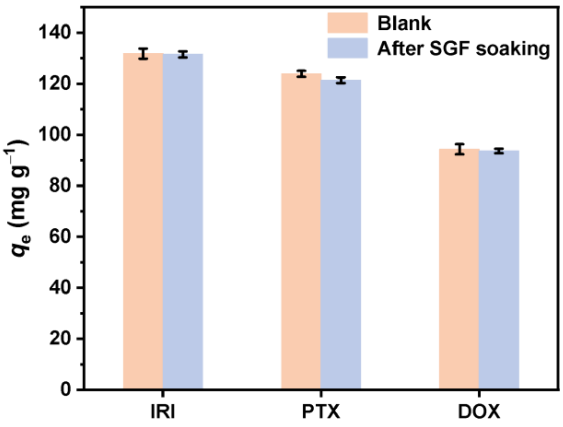

Fig. S31 Adsorption capacities of untreated and SGF-pretreated C4A-TAN (0.375 mg mL^{-1}) toward chemotherapeutic drugs (initial concentration: 50 μg mL^{-1}). SGF pretreatment was performed by immersing 4.5 mg of the adsorbent in 12.0 mL of SGF at room temperature for 2.0 h (close to the normal gastric emptying time of drugs), followed by centrifugal separation.

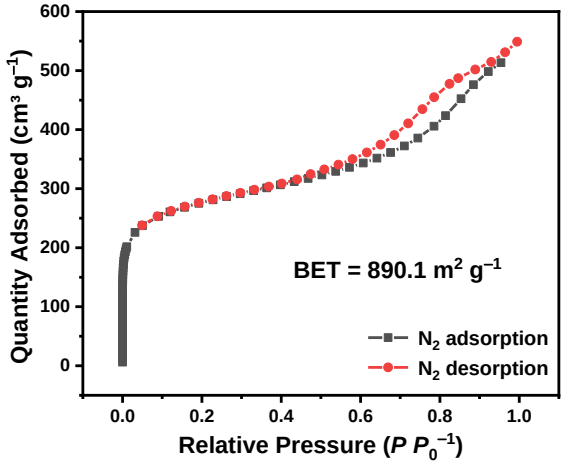

Fig. S32 N_2 adsorption–desorption isotherm for MAC measured at 77 K.

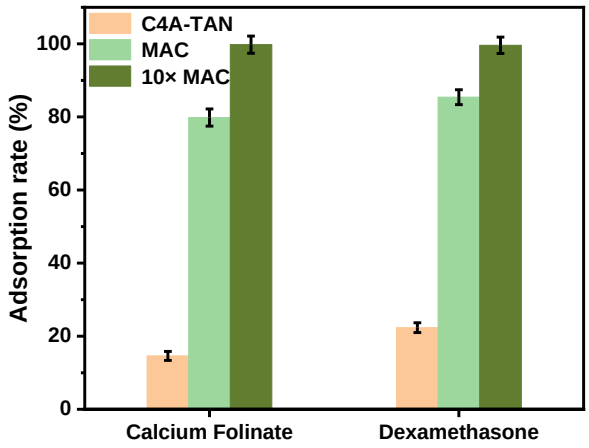

Fig. S33 Adsorption rates of adjuvant drugs (calcium folinate and dexamethasone, C_0 = 50 mg L^{-1}) after adsorption by C4A-TAN (0.375 mg mL^{-1}) and MAC (0.375 and 3.75 mg mL^{-1}).

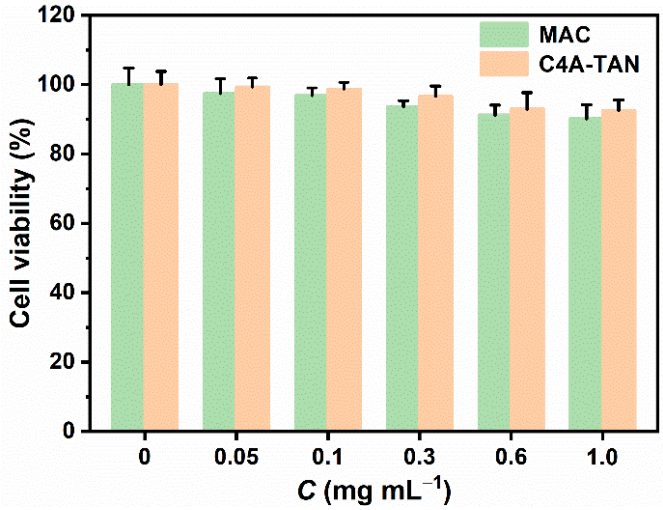

Fig. S34 Cytotoxicity of C4A-TAN and MAC in MODE-K cells. Cell viability was assessed after 24 h of exposure to increasing concentrations (0–1.0 mg·mL^{-1}) of the adsorbents.

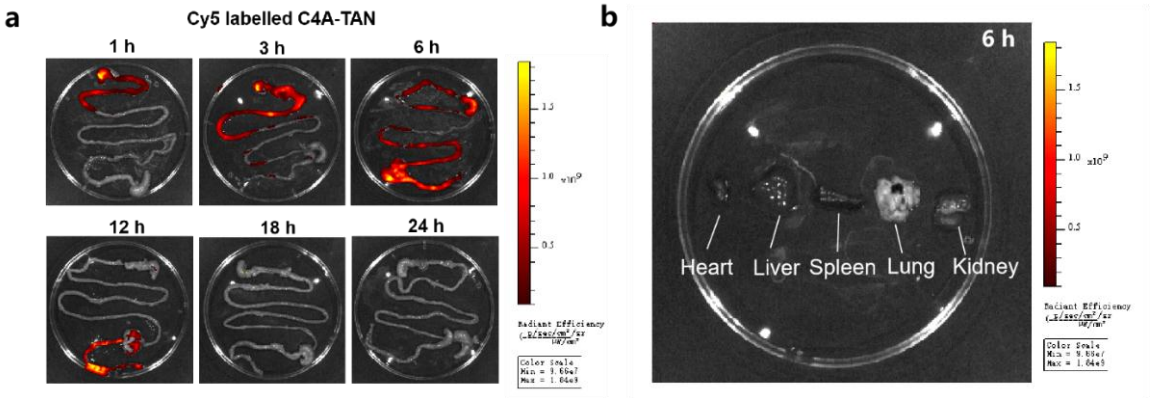

Fig. S35 Fluorescence images of (a) the gastrointestinal tract and (b) other major organs from mice following oral administration of Cy5-labeled C4A-TAN (750 mg kg^{-1}).

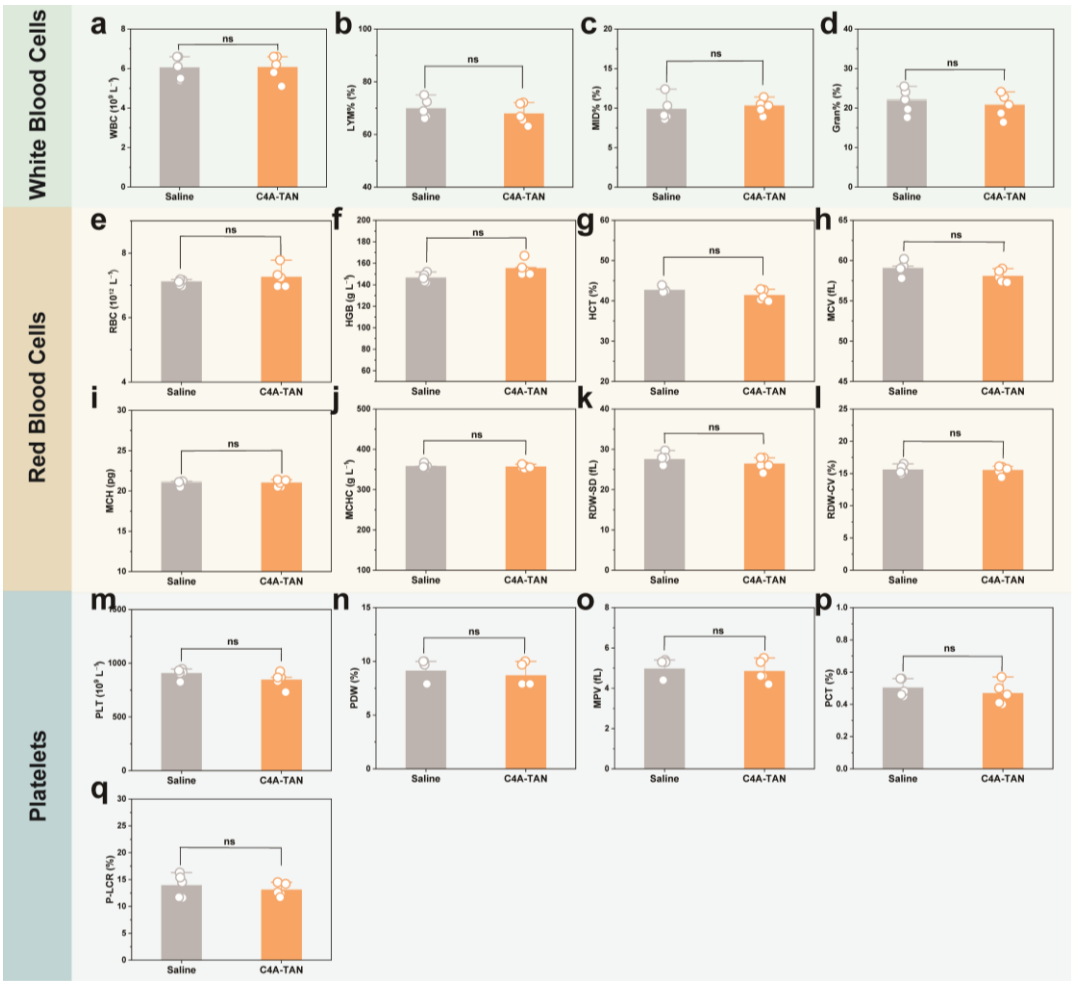

Fig. S36 Complete blood count analysis of mice treated with C4A-TAN or saline (control). The following parameters were evaluated: (a) white blood cell count (WBC); (b) lymphocyte percentage (LYM%); (c) mid-range cell percentage (MID%); (d) granulocyte percentage (Gran%); (e) red blood cell count (RBC); (f) hemoglobin concentration (HGB); (g) hematocrit (HCT); (h) mean corpuscular volume (MCV); (i) mean corpuscular hemoglobin (MCH); (j) mean corpuscular hemoglobin concentration (MCHC); (k) red cell distribution width–standard deviation (RDW-SD); (l) red cell distribution width–coefficient of variation (RDW-CV); m) platelet count (PLT); (n) platelet distribution width (PDW); (o) mean platelet volume (MPV); (p) plateletcrit (PCT); and (q) platelet–large cell ratio (P-LCR).

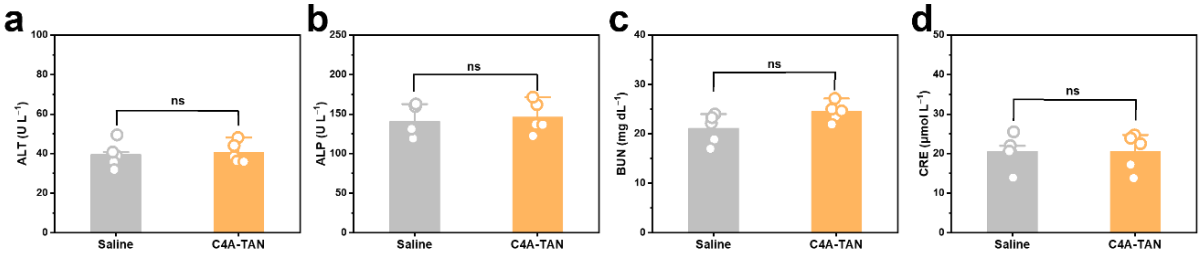

Fig. S37 Serum biochemistry analysis of liver and kidney functions in mice treated with C4A-TAN or saline (control). Liver function markers: (a) alanine aminotransferase (ALT) and (b) alkaline phosphatase (ALP). Renal function parameters: (c) blood urea nitrogen (BUN) and (d) creatinine (CRE).

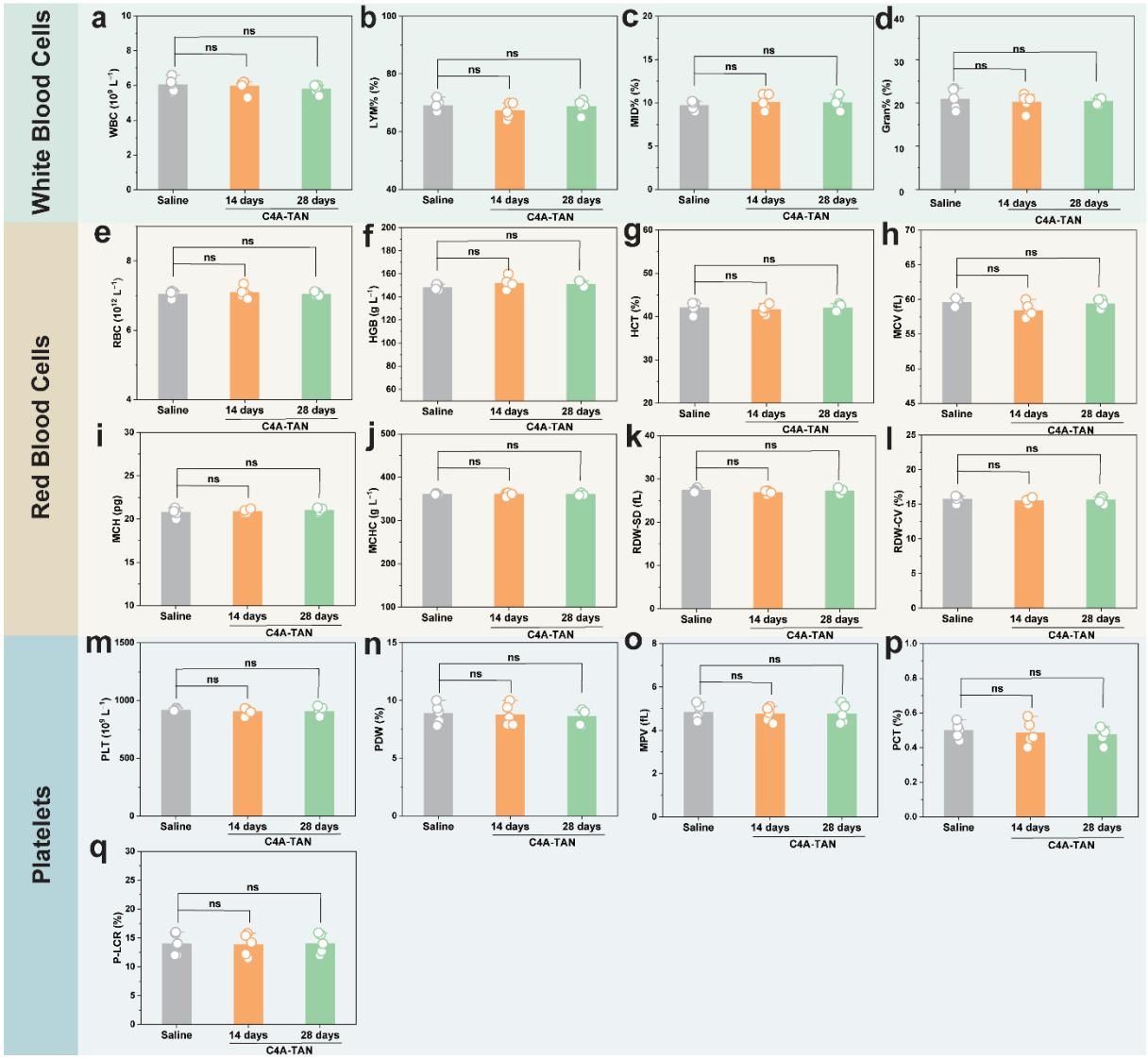

Fig. S38 Complete blood count analysis of mice after 14 and 28 days of repeated C4A-TAN administration, compared with saline-treated controls at 28 days. The following parameters were evaluated: (a) white blood cell count (WBC); (b) lymphocyte percentage (LYM%); (c) mid-range cell percentage (MID%); (d) granulocyte percentage (Gran%); (e) red blood cell count (RBC); (f) hemoglobin concentration (HGB); (g) hematocrit (HCT); (h) mean corpuscular volume (MCV); (i) mean corpuscular hemoglobin (MCH); (j) mean corpuscular hemoglobin concentration (MCHC); (k) red cell distribution width–standard deviation (RDW-SD); (l) red cell distribution width–coefficient of variation (RDW-CV); m) platelet count (PLT); (n) platelet distribution width (PDW); (o) mean platelet volume (MPV); (p) plateletcrit (PCT); and (q) platelet–large cell ratio (P-LCR).

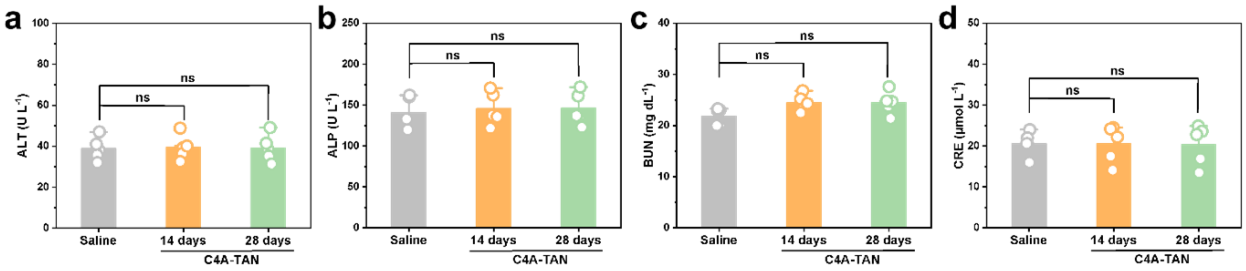

Fig. S39 Serum biochemical analysis of liver and kidney functions in mice after 14 and 28 days of repeated C4A-TAN administration, compared with saline-treated controls at 28 days. Liver function markers: (a) alanine aminotransferase (ALT) and (b) alkaline phosphatase (ALP). Renal function parameters: (c) blood urea nitrogen (BUN) and (d) creatinine (CRE).

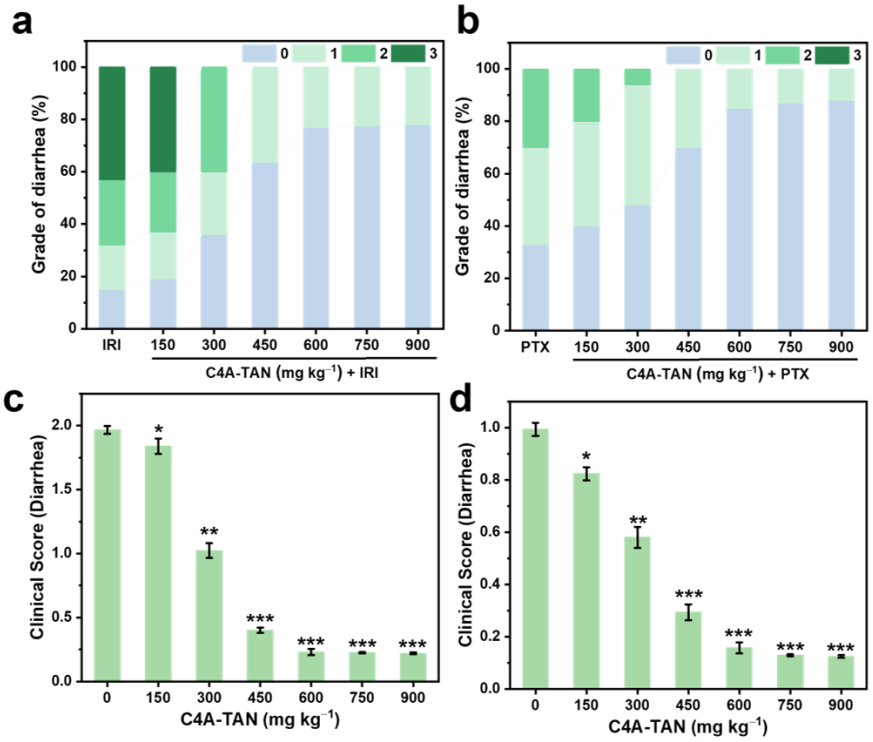

Fig. S40 Diarrhea severity in mice treated with (a) IRI and (b) PTX following administration of varying doses of C4A-TAN, evaluated using a stool consistency scoring system (0, normal; 1, mild [loose stool]; 2, moderate [unformed stool]; 3, severe [watery stool]). Weighted mean diarrhea scores for the groups treated with (c) IRI + C4A-TAN and (d) PTX + C4A-TAN, calculated based on the severity distribution. Data are presented as mean ± standard error (n = 5).

Supporting tables

Table S1 Optimization of the synthetic conditions for the olefin-linked C4A-based POPs

POPs	Solvent	*t* (°C)	Results
C4A-TAN	1,4-dioxane/KOH = 9:1	120	Starting material
	1,4-dioxane/Mes/KOH = 8:1:1	120	Starting material
	1,4-dioxane/Mes/KOH = 6:3:1	120	Starting material
	1,4-dioxane/Mes/KOH = 5:4:1	120	Starting material
	1,4-dioxane/MeCN/KOH = 8:1:1	120	Starting material
	1,4-dioxane/Mes/MeOH/KOH = 6:1:2:1	120	Starting material
	1,4-dioxane/MeOH/KOH = 8:1:1	120	Starting material
	DMF/KOH = 9:1	120	No solid
	1,4-dioxane/DMF/KOH = 8:1:1	120	Starting material
	1,4-dioxane/DMF/MeOH/KOH = 1:5:3:1	150	No solid
	1,4-dioxane/DMF/MeOH/KOH = 5:1:3:1	150	Little solid
	1,4-dioxane/MeOH/MeCN/KOH = 3:3:3:1	150	Little solid
	1,4-dioxane/MeOH/MeCN/KOH = 4:4:1:1	150	Little solid
	1,4-dioxane/DMF/MeOH/MeCN/KOH = 4:3:1:1:1	150	Little solid
	1,4-dioxane/DMF/MeOH/MeCN/KOH = 2:3:2:2:1	150	Large amount of solid
C4A-PAN	1,4-dioxane/DMF/MeOH/MeCN/KOH = 2:3:2:2:1	150	Large amount of solid
C4A-BAN	1,4-dioxane/DMF/MeOH/MeCN/KOH = 2:3:2:2:1	150	Large amount of solid
C4A-QAN	1,4-dioxane/DMF/MeOH/MeCN/KOH = 2:3:2:2:1	150	Large amount of solid

Table S2 Fitting parameters of the Langmuir model for the equilibrium adsorption of chemotherapeutic drugs on POPs.

Drug	Adsorbent	Q_{max} (mg g^{-1})	K_L (L mg^{-1})	K_L (M^{-1})	R^2
IRI	C4A-PAN	50.1	1.933	1.31×10^6	0.9858
	C4A-BAN	329.9	1.593	1.08×10^6	0.9867
	C4A-TAN	330.7	2.833	1.92×10^6	0.9880
	C4A-QAN	316.5	1.308	8.85×10^5	0.9947
PTX	C4A-PAN	59.1	0.072	6.14×10^4	0.9907
	C4A-BAN	250.6	0.086	7.36×10^4	0.9824
	C4A-TAN	279.3	0.184	1.57×10^5	0.9902
	C4A-QAN	253.7	0.075	6.36×10^4	0.9892
DOX	C4A-PAN	26.0	0.114	6.60×10^4	0.9900
	C4A-BAN	43.1	0.124	7.17×10^4	0.9894
	C4A-TAN	224.6	0.274	1.61×10^5	0.9836
	C4A-QAN	163.9	0.143	8.30×10^4	0.9972

Table S3 Fitting parameters of the Freundlich model for the equilibrium adsorption of chemotherapeutic drugs on POPs.

Drug	Adsorbent	K_F (mg g^{-1})	1/n	R^2
IRI	C4A-PAN	28.9	0.1707	0.9535
	C4A-BAN	179.8	0.1786	0.9613
	C4A-TAN	200.2	0.1511	0.9403
	C4A-QAN	170.7	0.1724	0.9498
PTX	C4A-PAN	13.7	0.2885	0.9485
	C4A-BAN	45.7	0.3602	0.9243
	C4A-TAN	76.3	0.2946	0.9548
	C4A-QAN	41.9	0.3768	0.9175
DOX	C4A-PAN	7.5	0.2327	0.9840
	C4A-BAN	11.6	0.2485	0.9854
	C4A-TAN	59.0	0.2903	0.9553
	C4A-QAN	29.7	0.3465	0.9861

Table S4 Fitting parameters of the Sips model for the equilibrium adsorption of chemotherapeutic drugs on POPs.

Drug	Adsorbent	Q_e (mg g^{-1})	K_s (L mg^{-1})	m_S	R^2
IRI	C4A-PAN	53.4	1.723	0.918	0.9837
	C4A-BAN	346.4	1.380	0.954	0.9857
	C4A-TAN	349.4	3.156	0.924	0.9767
	C4A-QAN	321.7	1.263	0.901	0.9901
PTX	C4A-PAN	55.4	0.081	1.029	0.9882
	C4A-BAN	223.4	0.116	1.028	0.9768
	C4A-TAN	296.6	0.155	0.940	0.9853
	C4A-QAN	219.6	0.107	1.078	0.9876
DOX	C4A-PAN	29.8	0.073	0.941	0.9897
	C4A-BAN	47.4	0.088	0.905	0.9885
	C4A-TAN	215.6	0.383	1.068	0.9815
	C4A-QAN	183.4	0.081	0.958	0.9892

Table S5 Fitting parameters of the Redlich-Peterson model for the equilibrium adsorption of chemotherapeutic drugs on POPs.

Drug	Adsorbent	K_{RP} (L mg^{-1})	a_{RP} (mg^{-g} L^{g})	g	R^2
IRI	C4A-PAN	136.2	3.131	0.950	0.9825
	C4A-BAN	676.7	2.417	0.950	0.9856
	C4A-TAN	1355.5	4.818	0.950	0.9813
	C4A-QAN	442.6	1.471	0.985	0.9874
PTX	C4A-PAN	3.7	0.043	1.075	0.9871
	C4A-BAN	17.7	0.035	1.157	0.9814
	C4A-TAN	58.2	0.252	0.957	0.9837
	C4A-QAN	14.6	0.020	1.139	0.9811
DOX	C4A-PAN	5.8	0.445	0.972	0.9893
	C4A-BAN	9.3	0.407	0.980	0.9890
	C4A-TAN	61.1	0.262	1.008	0.9834
	C4A-QAN	25.9	0.208	0.941	0.9918

Table S6 Binding energy calculations ($\Delta E = E_{complex} - E_{host} - E_{guest}$ + BSSE) for C4A and its olefin-extended derivative with chemotherapeutic drugs[a]

Host	Guest	E_{host} (Hartree)	E_{guest} (Hartree)	$E_{complex}$ (Hartree)	BSSE (Hartree)	ΔE (Hartree)	ΔE (kJ mol^{-1})
C4A	IRI	−1382.6	−1951.7	−3334.3	0.01719	−0.0228	−59.9
	PTX		−2930.9	−4313.5	0.01151	−0.0185	−48.6
	DOX		−1929.3	−3311.9	0.01379	−0.0362	−95.1
C4A-CH=C(CN)Ph	IRI	−2986.5	−1951.7	−4938.2	0.02110	−0.0589	−154.6
	PTX		−2930.9	−5917.4	0.02021	−0.0698	−183.2
	DOX		−1929.3	−4915.9	0.02445	−0.1856	−487.2

[a] Performed at the B3LYP-D3/6-31G(d,p)//B3LYP-D3/6-311G(2df,2p) level using the SMD solvation model (water as solvent).

Table S7 Langmuir model Fitting parameters for the adsorption of chemotherapeutic drugs onto imine-, azo- and olefin-linked POPs.

Drug	Adsorbent	Q_{max} (mg g^{-1})	K_L (L mg^{-1})	R^2
IRI	C4A-TAN	330.7	2.833	0.9880
	C4A-C=N-TP	167.2	1.593	0.9781
	C4A-N=N-TP	133.6	1.068	0.9856
PTX	C4A-TAN	279.3	0.184	0.9902
	C4A-C=N-TP	80.0	0.051	0.9919
	C4A-N=N-TP	100.4	0.095	0.9877
DOX	C4A-TAN	224.6	0.274	0.9836
	C4A-C=N-TP	79.9	0.182	0.9866
	C4A-N=N-TP	94.2	0.162	0.9845

Table S8 Fitting parameters for the adsorption kinetics of chemotherapeutic drugs on the POPs

Drug	Adsorbent	Pseudo-First-Order Model		Pseudo-Second-Order Model	
		k_1 (min^{-1})	R^2	k_2 (g mg^{-1} min^{-1})	R^2
IRI	C4A-PAN	0.0325	0.9839	0.00304	0.9840
	C4A-BAN	0.0461	0.9594	0.00300	0.9972
	C4A-TAN	0.0365	0.9363	0.00444	0.9982
	C4A-QAN	0.0517	0.9833	0.00443	0.9985
PTX	C4A-PAN	0.0323	0.9765	0.00415	0.9854
	C4A-BAN	0.0507	0.9354	0.00674	0.9989
	C4A-TAN	0.0430	0.9164	0.00762	0.9990
	C4A-QAN	0.0469	0.9393	0.00520	0.9970
DOX	C4A-PAN	0.0352	0.8027	0.00464	0.9705
	C4A-BAN	0.0404	0.8283	0.00387	0.9711
	C4A-TAN	0.0424	0.8064	0.00421	0.9996
	C4A-QAN	0.0364	0.7029	0.00333	0.9996

Table S9 Comparison of adsorption rate constants for C4A-based POPs against reported adsorbents[a]

Drug	Adsorbent	k_2 (g·mg^{-1}·min^{-1})	Ref.
PTX	MCOF-TPB-MPA	0.005	7
	MCOF-TPB-PDA	0.003	7
	MCOF-TTA-PDA	0.003	7
	Fe_3O_4/MWCNT	0.0009	8
	Fe_3O_4/GO	0.0007	8
	C4A-PAN	0.0042	This work
	C4A-BAN	0.0067	This work
	C4A-TAN	0.0076	This work
	C4A-QAN	0.0052	This work
DOX	Fe_3O_4 NPs	0.00070	9
	GO-Fe_3O_4-PEG	0.00456	10
	GO-Fe_3O_4-PH	0.00775	10
	GO@Fe_3O_4@β-CD	0.00900	11
	Fe_3O_4@SiO_2-Glu	0.01550	12
	BFO nanoparticles	0.00009	13
	C4A-PAN	0.00421	This work
	C4A-BAN	0.00387	This work
	C4A-TAN	0.00464	This work
	C4A-QAN	0.00333	This work

[a] Because previous studies on adsorbents for IRI have not investigated adsorption kinetics, this drug is excluded from the comparison.

Table S10 Selectivity coefficients of C4A-TAN for chemotherapeutic drugs relative to various nutrients.

Nutrients	$q_{drug}/q_{nutrient}$	
	IRI	PTX
Glucose	478	242
Sucrose	446	364
Glycine	503	320
Serine	409	354
Cysteine	503	346
Proline	446	413
Oleic acid	434	404
Linoleic acid	516	200

References

1 M. Kandpal, A. K. Bandela, V. K. Hinge, V. R. Rao and C. P. Rao, *ACS Appl. Mater. Interfaces*, 2013, **5**, 13448–13456.
2 S. Li, L. Li, Y. Li, L. Dai, C. Liu, Y. Liu, J. Li, J. Lv, P. Li and B. Wang, *ACS Catal.*, 2020, **10**, 8717–8726.
3 T. Jia, C. Pu, T. Qin, B. Liu, G. Yao, Z. Xun, B. Wang, Y. Tian, Z. Zhang, H. Xu and C. Zhao, *J. Agric. Food Chem.*, 2022, **70**, 15981–15989.
4 B. Garai, D. Shetty, T. Skorjanc, F. Gándara, N. Naleem, S. Varghese, S. K. Sharma, M. Baias, R. Jagannathan, M. A. Olson, S. Kirmizialtin and A. Trabolsi, *J. Am. Chem. Soc.*, 2021, **143**, 3407–3415.
5 S. Pasquale, S. Sattin, E. C. Escudero-Adán, M. Martínez-Belmonte and J. de Mendoza, *Nat. Commun*., 2012, **3**, 785.
6 J. B. Maglic, R. Lavendomme, *J. Appl. Cryst.*, 2022, **55**, 1033–1044.
7 W. Li, Y. Sun, Y. Tang, Y. Ren and S. Wang, *Appl. Surf. Sci*., 2025, **686**, 162185.
8 S. Safari, F. Nasehi, E. Fataei, B. Khanizadeh and A. A. Imani, *Iran J Sci. Technol. Trans. Sci.*, 2022, **46**, 1583–1597.
9 X. Weng, L. Ma, M. Guo, Y. Su, R. Dharmarajan and Z. Chen, *Chem. Eng. J.*, 2018, **353**, 482–489.
10 M. Barzegarzadeh and M. S. Amini-Fazl, *J. Polym. Environ*., 2023, **31**, 177–192.
11 M. Ghafoori, M. Cheraghi, M. K. Sadr, B. Lorestani and S. Sobhanardakani, *Environ. Sci. Pollut. Res.*, 2022, **29**, 35012–35024.
12 W. Cai, M. Guo, X. Weng, W. Zhang and Z. Chen, *Mater. Sci. Eng. C.,* 2019, **98**, 65–73.
13 M. A. Abbasi, Z. Ali, Z. Qamar, K. Shahzad, H. K. Siddiqui, M. Atif, Z. Ali and W. Khalid, *Ceram. Int.*, 2021, **47**, 14390–14398.